Decomposition boundary from high-pressure clinoenstatite to wadsleyite + stishovite in MgSiO$_3$ ⚐

Shigeaki Ono[1],*, Takumi Kikegawa[2], and Yuji Higo[3]

[1]Research and Development Center for Ocean Drilling Science, Japan Agency for Marine-Earth Science and Technology, 2-15 Natsushima-cho, Yokosuka-shi, Kanagawa 237-0061, Japan
[2]High Energy Acceleration Research Organization, 1-1 Oho, Tsukuba 305-0801, Japan
[3]Japan Synchrotron Radiation Research Institute, Sayo-cho, Sayo-gun, Hyogo 679-5198, Japan

Abstract

The reaction boundary between high-pressure clinoenstatite and wadsleyite + stishovite in MgSiO$_3$ was investigated using a multi-anvil high-pressure apparatus and synchrotron X-ray diffraction. Experimental pressures were monitored via in situ powdered X-ray diffraction of gold, which was also put into the sample chamber. Stable phases at each pressure and temperature were confirmed by powdered X-ray diffraction data and observing the recovered samples. The reaction boundary was found to occur at P (GPa) = 16.1 + 0.0064 × (T − 1250) (K), where the pressure dependence of the slope of the reaction boundary, dP/dT, is similar to that of the phase boundary between wadsleyite and ringwoodite. Thus, the stability field of wadsleyite and stishovite expands to a low-temperature region, reconciling an inconsistency recorded between previous studies regarding the phase relation in MgSiO$_3$.

Keywords: Clinoenstatite, wadsleyite, stishovite, high pressure

Introduction

Because olivine, pyroxene, and garnet are major minerals in the upper mantle, understanding the latter's dynamics and evolution requires knowledge of MgSiO$_3$, which is an end-member of pyroxene. To this end, phase relations in MgSiO$_3$ have been repeatedly investigated by several authors (e.g., Kanzaki 1987; Sawamoto 1987; Ito and Takahashi 1989; Gasparik 1990; Pacalo and Gasparik 1990; Kanzaki 1991; Angel and Hugh-Jones 1994; Kato et al. 1995; Ono et al. 2001; Akashi et al. 2009; Stixrude and Lithgow-Bertelloni 2011; Jacobs et al. 2017). The transition sequence of the MgSiO$_3$ mineral along the normal mantle geotherm (Brown and Shankland 1981; Ono 2008) proceeds from low clinoenstatite to orthoenstatite and high-pressure clinoenstatite with an increase in pressure (Pacalo and Gasparik 1990; Kanzaki 1991; Angel and Hugh-Jones 1994). High-pressure clinoenstatite then decomposes to two phases of wadsleyite and stishovite at the bottom of the upper mantle (Kanzaki 1987; Sawamoto 1987), which in turn changes to a single phase of akimotoite (Sawamoto 1987; Gasparik 1990) followed by bridgmanite at the bottom of the transition zone (Ito and Takahashi 1989; Kato et al. 1995; Ono et al. 2001). The stability field of ringwoodite and stishovite is lower than the normal mantle geotherm (Ono et al. 2017). In the case of a low-temperature path, such as the pressure-temperature conditions of the subducted slab, the appearance of a stability field of wadsleyite + stishovite remains as yet unconfirmed. Whereas some previous studies have reported that the two phases of ringwoodite + stishovite are stable rather than wadsleyite + stishovite (Ito and Navrotsky 1985; Gasparik 1990), others have proposed that the two phases of wadsleyite + stishovite are stable between the stability fields of high-pressure clinoenstatite and ringwoodite + stishovite (Sawamoto 1987; Stixrude and Lithgow-Bertelloni 2011; Jacobs et al. 2017). This discrepancy among researchers is likely due to the accuracy of phase boundary determination between high-pressure clinoenstatite and wadsleyite + stishovite.

In the present study, the use of a multi-anvil high-pressure system combined with a synchrotron radiation source enabled the acquisition of precise experimental pressures data from samples under high-pressure and high-temperature conditions. Herein, we report on the disputed issue of the phase boundary between high-pressure clinoenstatite and wadsleyite + stishovite in MgSiO$_3$, and we suggest a revised phase diagram for MgSiO$_3$ based on the obtained data.

Methods

High-pressure experiments were carried out using multi-anvil high-pressure apparatus installed at the synchrotron facilities of KEK and SPring-8 in Japan. These systems were equipped with an energy-dispersive X-ray diffractometer with a germanium solid-state detector. Tungsten carbide cubic anvils were truncated at one corner to accommodate an octahedral pressure medium containing the sample and heater. Three sizes of truncation were adopted: 3 mm for experiments involving low pressures and temperatures, and 2 and 1.5 mm for those involving high pressures and temperatures. Anvil breakage was prevented by separating them with pyrophyllite gaskets and balsa wood spacers. Semi-sintered magnesia (MgO) octahedra were used as the pressure-transmitting medium. Heating assemblies were similar to those reported in previous studies (Ono et al. 2011, 2013), comprising a heating unit composed of TiB$_2$ + B (Ono 2016), with the tube placed at the center of the pressure-transmitting medium. The ZrO$_2$ sleeve outside the heater served as thermal insulation. The X-ray diffractometer system included incident (white) and diffracted X-ray beams of 50 μm width, with a diffraction angle of 2θ = 6.0°.

A synthetic MgSiO₃ gel was used as the starting material in the experiments based on its homogeneous and reactive properties that enabled the rapid achievement of an equilibrium state (e.g., Hamilton and Henderson 1968; Ono and Yasuda 1996). A mixture of the powdered MgSiO₃ and gold, which was used as a pressure standard, was loaded into the heater sleeve, which also served as the sample capsule. The sample temperature was monitored using a $W_{97}Re_3$-$W_{75}Re_{25}$ thermocouple inserted at the center of the sample capsule; no correction was made to counter the effect of pressure on the thermocouple EMF. Temperature fluctuation during heating was within ±10 °C. X-ray measurements of the sample were taken close to the thermocouple junction (<50 μm), which indicated that the temperature gradient between the X-ray position and the thermocouple junction was kept to within 50 °C. The temperature was maintained for 2–4 h. Experimental pressures were determined from the unit-cell volumes of gold using the appropriate equation of state (Dorogokupets and Dewaele 2007). The typical uncertainty in the pressure estimation was 0.2–0.3 GPa. After being kept at the desired pressure and temperature for the desired duration, samples were quenched by cutting off the electric power supply. After the termination of heating, the pressure decreased slowly and the sample could be removed. All recovered samples were polished prior to investigation with an electron microprobe analyzer (JXA-8500F, JEOL), with the stable phase in each experimental run determined based on the chemical composition of phases in the recovered sample. As it was difficult to identify wadsleyite or ringwoodite by observing chemical compositions, the powdered X-ray diffraction data were also used to identify stable phases.

RESULTS

After reaching the desired pressure at ambient temperature, the sample temperature was quickly increased to the desired temperature. As the temperature increased, the X-ray diffraction peaks of gold became sharp at around 1000 K, indicating that the recrystallization of gold had commenced and that the differential stress in the sample chamber was gradually released. After the desired temperature was reached, the measurement of pressure started and continued until temperature quenching. The typical pressure fluctuation was ~0.2 GPa, which was consistent with a value observed in previous study using the similar cell assembly (Ono et al. 2013).

Twelve runs were performed at pressures between 15 and 19 GPa (Table 1). The powder X-ray diffraction peaks of gold were sufficiently intense to calculate the experimental pressures, with Figure 1 showing the typical X-ray diffraction data acquired at 17.1 GPa and 1200 K. In addition to the gold peaks, some peaks associated with TiB₂ and MgO were also observed reflecting their use as the heater and pressure-transmitting medium, respectively. Figure 2 shows typical quenched sample images obtained using the electron microprobe analyzer. At pressures below the reaction boundary, the MgSiO₃ starting material changed to a single phase of high-pressure clinoenstatite, represented by the gray phase (MgSiO₃) in Figure 2a. In contrast, at pressures higher than the reaction boundary the starting material changed to Mg-rich and silica phases (Fig. 2b), with the chemical compositions of
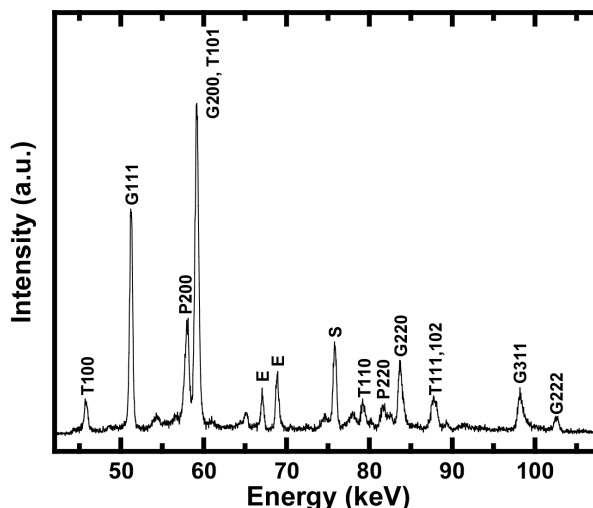

FIGURE 1. Example X-ray diffraction pattern acquired at 17.1 GPa and 1200 K. Key to label abbreviations: G = gold (Au); E = emission of gold fluorescence; T = TiB₂; P = periclase (MgO); and S = unidentified spot peak.
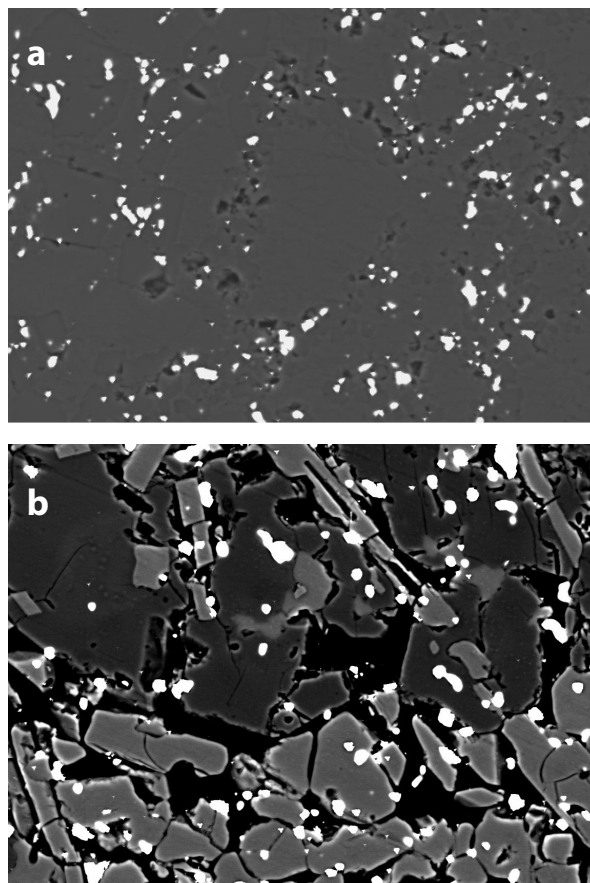

FIGURE 2. Example backscattered electron microphotographs of quenched sample conditions. (**a**) White areas are the gold phase used as the pressure reference, while the gray and black areas are MgSiO₃ and voids, respectively. Horizontal scale 100 μm, experimental conditions 1200 K and 15.3 GPa. (**b**) White and black areas are the gold and the void, respectively, and dark and light grays are Mg₂SiO₄ and SiO₂, respectively. Horizontal scale 120 μm. The experimental conditions 1350 K and 17.3 GPa.

TABLE 1. Experimental conditions and results

T (K)	P (GPa)	t (h)	Phases present
1150	15.0(2)	4.0	MgSiO₃
1200	15.3(3)	3.0	MgSiO₃
1200	17.1(2)	2.0	Mg₂SiO₄ (ringwoodite) + SiO₂
1250	15.6(5)	2.0	Mg₂SiO₄ + SiO₂
1300	15.0(3)	2.0	MgSiO₃
1300	16.5(2)	4.0	Mg₂SiO₄ (wadsleyite) + SiO₂
1300	18.1(2)	4.0	Mg₂SiO₄ (ringwoodite) + SiO₂
1300	18.7(1)	2.0	Mg₂SiO₄ (ringwoodite) + SiO₂
1300	18.9(3)	2.0	Mg₂SiO₄ + SiO₂
1350	16.7(3)	2.0	MgSiO₃
1350	17.3(3)	2.0	Mg₂SiO₄ (wadsleyite) + SiO₂
1400	18.1(6)	2.0	Mg₂SiO₄ (wadsleyite) + SiO₂

Note: T, P, and t are the temperature, pressure, and heating duration, respectively.

the light- and dark-gray phases being pure SiO_2 and Mg_2SiO_4, respectively. According to previous study (Suzuki et al. 2000), the Mg_2SiO_4 phase observed in our recovered samples might be wadsleyite or ringwoodite. However, it was difficult to identify the Mg_2SiO_4 phase from its chemical composition. Therefore, week diffraction peaks associated with the sample were investigated to identify the Mg_2SiO_4 phase (Fig. 3).

The pressure-temperature conditions of the acquired X-ray diffraction patterns of gold and the stable phases identified in the quenched samples are shown in Figure 4. The gradient of dP/dT of the reaction boundary is positive, with the transition boundary shown in Figure 4 expressed by the following linear equation:

$$P \text{ (GPa)} = 16.1(3) + 0.0064(15) \times (T - 1250) \text{ (K)}.$$

The boundary determined in this study is in general agreement with that reported elsewhere (Sawamoto 1987; Stixrude and Lithgow-Bertelloni 2011; Jacobs et al. 2017).

DISCUSSION

Previous studies (Ito and Navrotsky 1985; Gasparik 1990) have reported that the reaction boundary between high-pressure clinoenstatite and wadsleyite + stishovite has a shallow dP/dT slope compared with that of the wadsleyite-ringwoodite boundary, with the triple point of high-pressure clinoenstatite-

wadsleyite + stishovite-ringwoodite + stishovite appearing at around 1000 K. Thus, the stability field of wadsleyite + stishovite was not observed at temperatures lower than ~1000 K. In contrast, the slope of this reaction boundary determined in our study was almost equal to that of the wadsleyite-ringwoodite boundary (Suzuki et al. 2000), in general agreement with the findings reported by Sawamoto (1987). This discrepancy can largely be explained by the influence of the chemical reaction kinetics on the determination of the reaction boundary, which is significant at low temperatures. Any uncertainty in the identification of stable phases might thus lead to discrepancies between different dP/dT slopes. It is known that a use of both forward and reverse experiments is suitable to determine the equilibrium boundary. However, it is difficult to use this method at low temperatures in the $MgSiO_3$ system (Gasparik 1989). In our study, therefore, synthetic gel was used as the starting material to enhance the chemical reaction at low temperatures because it is more reactive than the oxide mixtures or crystals used in previous studies.

However, although the dP/dT slope reported by Sawamoto (1987) was consistent with that determined here, the pressure recorded in the earlier work was 2 GPa higher than that obtained in our study. Furthermore, the pressure of the wadsleyite-ringwoodite boundary reported by Sawamoto (1987) was also 1.5 GPa higher than that reported by Suzuki et al. (2000). Significantly, Sawamoto (1987) used the conventional quench method in his high-pressure experiments, which produces considerable uncertainty in terms of experimental pressure. Furthermore, as the pressure generation efficiency of the employed high-pressure apparatus was calibrated using several fixed pressure points prior
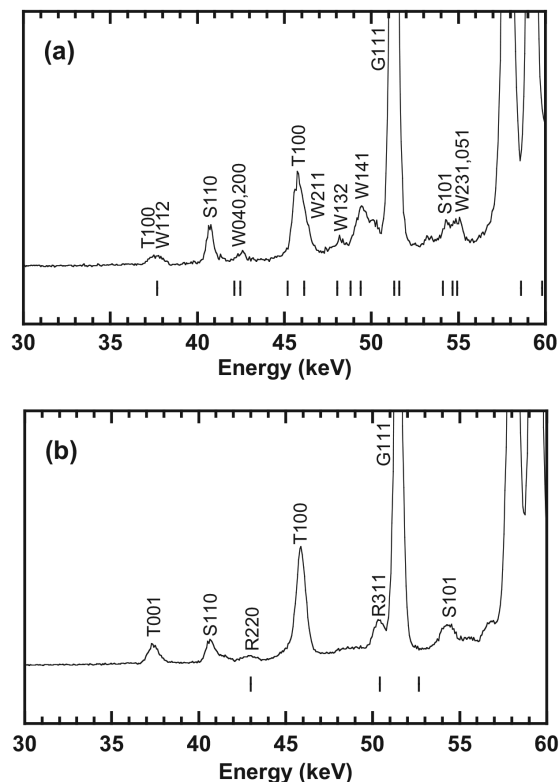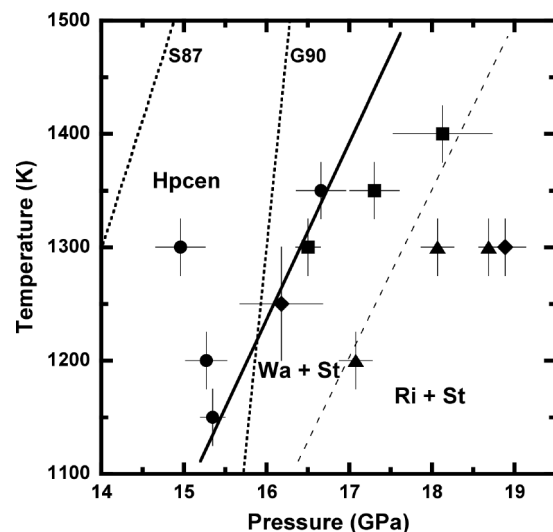
FIGURE 3. X-ray diffraction patterns acquired where wadsleyite or ringwoodite was stable. (a) Wadsleyite was identified. (b) Ringwoodite was identified. Key to label abbreviations: G = gold (Au); T = TiB₂; S = stishovite (SiO₂); W= wadsleyite (Mg₂SiO₄); and R = ringwoodite (Mg₂SiO₄). Vertical bars denote the calculated diffraction peaks of wadsleyite (a) or ringwoodite (b).

FIGURE 4. Experimental results and reaction boundary between high-pressure clinoenstatite and wadsleyite + stishovite in MgSiO₃. Circles, squares, and triangles denote the stability conditions of single phase MgSiO₃, Mg₂SiO₄ wadsleyite, and SiO₂ stishovite, and Mg₂SiO₄ ringwoodite and SiO₂ stishovite, respectively. Diamonds denote the two phases of SiO₂ and Mg₂SiO₄, which structure could not be identified by X-ray diffraction data because diffraction peaks from the sample were unclear. The solid and dot lines show the reaction boundary determined in our and previous studies (S87 = Sawamoto 1987; G90 = Gasparik 1990). The dashed line is the wadsleyite-ringwoodite boundary (Suzuki et al. 2000).
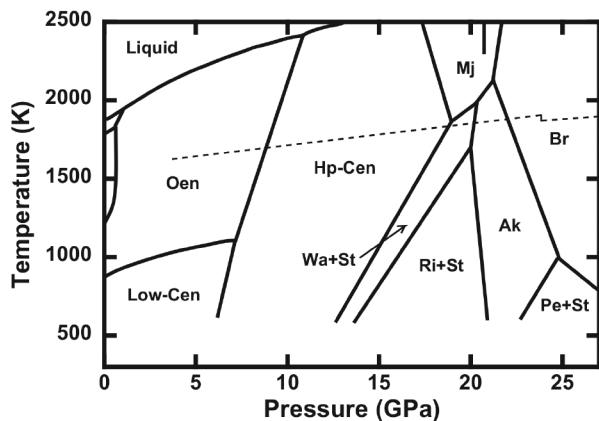
FIGURE 5. Phase diagram of MgSiO₃ estimated based the present and previous studies. Abbreviations: Low-Cen = low clinoenstatite; Oen = orthoenstatite; Hp-Cen = high-pressure clinoenstatite; Wa = wadsleyite; Ri = ringwoodite; St = stishovite; Mj = majorite; Ak = akimotoite; Br = bridgmanite; Pe = periclase. Dashed line shows the typical mantle geotherm (Ono 2008).

to the experiments, it was impossible to carry out in situ measurements of pressure values. In contrast, both the present study and that of Suzuki et al. (2000) involved the in situ monitoring of experimental conditions, using synchrotron radiation X-rays to determine accurate pressure values. In the case of phase boundary between wadsleyite and ringwoodite, our observations were in agreement with those reported by Suzuki et al. (2000).

IMPLICATIONS

Our new phase diagram for MgSiO₃ (Fig. 5) shows that the triple point of high-pressure clinoenstatite-wadsleyite + stishovite-ringwoodite + stishovite does not appear under mantle conditions, even considering the low-temperature P-T path in a subducted slab. This is consistent with the phase relation in MgSiO₃ estimated in previous studies based on thermodynamic analysis (Stixrude and Lithgow-Bertelloni 2011; Jacobs et al. 2017). Because the normal mantle geotherm (Brown and Shankland 1981; Ono 2008) is located between two triple points—high-pressure clinoenstatite–wadsleyite + stishovite–majorite and wadsleyite + stishovite–ringwoodite + stishovite–akimotoite—the transition sequence of MgSiO₃ in the transition zone is from high-pressure clinoenstatite to wadsleyite + stishovite, akimotoite, and finally to bridgmanite. In the case of low-temperature P-T paths, such as a subducted slab, the field of ringwoodite + stishovite appears between the fields of wadsleyite + stishovite and akimotoite, while in the case of high-temperature P-T paths, such as an upwelling mantle plume, the field of majorite appears at the high-pressure side of the field of high-pressure clinoenstatite.

REFERENCES CITED

Akashi, A., Nishihara, Y., Takahashi, E., Nakajima, Y., Tange, Y., and Funakoshi, K. (2009) Orthoenstatite/clinoenstatite phase transformation in MgSiO₃ at high-pressure and high-temperature determined by in situ X-ray diffraction: implications for nature of the X discontinuity. Journal of Geophysical Research, 114, B04206. doi: 10.1029/2008JB005894.

Angel, R.J., and Hugh-Jones, D.A. (1994) Equations of state and thermodynamic properties of enstatite pyroxenes. Journal of Geophysical Research, 99, 19,777–19,783.

Brown, J.M., and Shankland, T.J. (1981) Thermodynamic parameters in the Earth as determined from seismic profiles. Geophysical Journal of the Royal Astronomical Society, 66, 579–596.

Dorogokupets, P.I., and Dewaele, A. (2007) Equations of state of MgO, Au, Pt, NaCl-B1, and NaCl-B2: Internally consistent high-temperature pressure scales. High Pressure Research, 27, 431–446. doi: 10.1080/08957950701659700.

Gasparik, T. (1989) Transformation of enstatite – diopside – jadeite pyroxenes to garnet. Contributions to Mineralogy and Petrology, 102, 389–405.

——— (1990) Phase relations in the transition zone. Journal of Geophysical Research, 95, 15,751–15,769.

Hamilton, D.H., and Henderson, C.M.B. (1968) The preparation of silicate composition by a gelling method. Mineralogical Magazine, 36, 832–838.

Ito, E., and Navrotsky, A. (1985) MgSiO₃ ilmenite: Calorimetry, phase equilibria, and decomposition at atmospheric pressure. American Mineralogist, 70, 1020–1026.

Ito, E., and Takahashi, E. (1989) Postspinel transitions in the system Mg₂SiO₄-Fe₂SiO₄ and some geophysical implications. Journal of Geophysical Research, 94, 10637–10646.

Jacobs, M.H.G., Schmid-Fetzer, R., and van den Berg, A.P. (2017) Phase diagrams, thermodynamic properties and sound velocities derived from a multiple Einstein method using vibrational densities of states: an application to MgO–SiO₂. Physics and Chemistry of Minerals, 44, 43–62. doi: 10.1007/s00269-016-0835-4.

Kanzaki, M. (1987) Ultrahigh-pressure phase relations in the system Mg₄Si₄O₁₂-Mg₃Al₂Si₃O₁₂. Physics of the Earth and Planetary Interiors, 49, 168–175.

——— (1991) Ortho/clinoenstatite transition. Physics and Chemistry of Minerals, 17, 726–730.

Kato, T., Ohtani, E., Morishima, H., Yamazaki, D., Suzuki, A., Suto, M., Kubo, T., Kikegawa, T., and Shimomura, O. (1995) In situ X ray observation of high-pressure phase transitions of MgSiO₃ and thermal expansion of MgSiO₃ perovskite at 25 GPa by double-stage multianvil system. Journal of Geophysical Research, 100, 20,475–20,481.

Ono, S., and Yasuda, A. (1996) Compositional change of majoritic garnet in a MORB composition from 7 to 17 GPa and 1400 to 1600 °C. Physics of the Earth and Planetary Interiors, 96, 171–179.

Ono, S., Katsura, T., Ito, E., Kanzaki, M., Yoneda, A., Walter, M.J., Urakawa, S., Utsumi, W., and Funakoshi, K. (2001) In situ observation of ilmenite-perovskite phase transition in MgSiO₃ using synchrotron radiation. Geophysical Research Letters, 28, 835–838.

Ono, S. (2008) Experimental constraints on the temperature profile in the lower mantle. Physics of the Earth and Planetary Interiors, 170, 267–273. doi: 10.1016/j.pepi.2008.06.033.

——— (2016) P-V-T relations of titanium boride, TiB₂, determined using in-situ X-ray diffraction. Heliyon, 2, e00220. doi: 10.1016/j.heliyon.2016.e00220.

Ono, S., Kikegawa, T., and Higo, Y. (2011) In situ observation of a garnet-perovskite transition in CaGeO₃. Physics and Chemistry of Minerals, 38, 735–740. doi: 10.1007/s00269-011-0446-z.

——— (2013) In situ observation of a phase transition in Fe₂SiO₄ at high pressure and high temperature. Physics and Chemistry of Minerals, 40, 811–816. doi: 10.1007/s00269-013-0615-3.

Ono, S., Kikegawa, T., and Higo, Y. (2017) Reaction boundary between akimotoite and ringwoodite + stishovite in MgSiO₃. Physics and Chemistry of Minerals, 44, 425–430. doi: 10.1007/s00269-016-0869-7.

Pacalo, R.E.G., and Gasparik, T. (1990) Reversals of the orthoenstatite-clinoenstatite transition at high pressures and high temperatures. Journal of Geophysical Research, 95, 15,853–15,858.

Sawamoto, H. (1987) Phase diagram of MgSiO₃ at pressures up to 24 GPa and temperatures up to 2200°C: phase stability and properties of tetragonal garnet. In M.H. Manfhnani and Y. Syono, Eds., High-Pressure Research in Mineral Physics, p. 209–219. Terra-Pub, Tokyo.

Stixrude, L., and Lithgow-Bertelloni, C. (2011) Thermodynamics of mantle minerals—II. Phase equilibria. Geophysical Journal International, 184, 1180–1213. doi: 10.1111/j.1365-246X.2010.04890.x.

Suzuki, A., Ohtani, E., Morishima, H., Kubo, T., Kanbe, Y., Kondo, T., Okada, T., Terasaki, H., Kato, T., and Kikegawa, T. (2000) In situ determination of the boundary between wadsleyite and ringwoodite in Mg₂SiO₄. Geophysical Research Letters, 27, 803–806.